Mini-review

Received: 16 October 2023 Revised: 27 March 2024 Accepted article published: 29 March 2024 Published online in Wiley Online Library:

(wileyonlinelibrary.com) DOI 10.1002/pi.6636

3D printing of hybrid solid–liquid structures

Chia-Min Hsieh,[a†] Ciera E. Cipriani[b†] and Emily B. Pentzer[a,b*]

Abstract

3D printing is a versatile technology for creating objects with custom geometries and compositions and is increasingly employed for fabricating hybrid solid–liquid composites (SLCs). These composites, comprising solid matrices with integrated liquid components, showcase unique properties such as enhanced flexibility and improved thermal and electrical conductivities. This review focuses on methods to fabricate SLCs directly by different 3D printing techniques, e.g. without needing to backfill or impregnate a porous matrix. The techniques of extrusion, vat photopolymerization and material jetting combined with microfluidics, inkjet printing, vacuum filling and ultraviolet light curing to produce SLCs are emphasized. We also discuss the development of feedstocks, focusing on emulsions and polymer capsules as fillers, and analyze current literature to highlight their significance. The review culminates in a perspective on new directions, highlighting the potential of bicontinuous interfacially jammed emulsion gels (bijels) to facilitate the printing of continuous liquid pathways, alongside the importance of understanding ink formulation and stability. Concluding with future perspectives, we underline the transformative impact of 3D-printed SLCs in diverse applications, signaling a significant advancement in the field.

Keywords: 3D printing; solid–liquid structures; hybrid composites; co-printing; emulsions; capsules

INTRODUCTION

Solid–liquid composites (SLCs) are an intriguing class of materials consisting of solid matrices with liquid-filled pockets.[1] These composites embody a synergy of solid and liquid components, endowing them with unique properties unattainable by either constituent alone. SLCs can exhibit extraordinary flexibility, tunability and functionality, such as enhanced thermal and electrical conductivity and mechanical properties.[2,3] For example, liquid metals (LMs) coated with a silicone shell show extrinsic shape memory resulting from the phase transition of the LM and the deformability of the elastomer.[4] SLCs have been prevalently applied across electronics,[5–8] robotics,[5,9,10] microfluidics,[11,12] the food industry[13–19] and biotechnology.[19–21] According to a comprehensive review by Style *et al.*, those materials are traditionally fabricated via emulsion-templating, phase separation, and wetting and printing.[3] Emulsion-templating involves the solidification of one component of an emulsion to create the composite material, such as dispersing LM droplets in a heat-curable prepolymer, for example.[22] Second, phase separation can be induced by changes in environmental factors like temperature, affecting the interaction between miscible materials. This is demonstrated by saturating a silicone gel, a crosslinked polymer network swollen in silicone oil, with fluorinated oil and then reducing the temperature, which leads to the formation of droplets due to the decreased solubility of the oil in the gel at lower temperatures.[23] The last method is wetting and printing, which involves adding liquids to preformed solids or printing liquids on different substrates, such as LMs, with electric fields applied.[24] However, the geometries that emulsion-templating and phase separation can create are limited to mold shapes, whereas the wetting and printing discussed in the previous review focus more on multi-step processes.[3] Therefore, single-step approaches to realizing SLCs with customizable and intricate structures are worth developing and discussing.

Among the known fabrication techniques, 3D printing (3DP) stands out for its capability to rapidly fabricate structures with customized (e.g. implants and prosthetics) and complex (porous and lattice) geometries with reduced material waste,[25] which were unattainable via traditional techniques like molding and machining. Furthermore, research has demonstrated that 3DP can still create products with good mechanical strength comparable to conventional methods.[26] More importantly, 3DP offers the possibility of integrating solid and liquid phases in a single fabrication step, allowing for the creation of SLCs with tailored liquid distributions within the solid matrix. This integration is not just limited to combining traditional methods like emulsion-templating and phase separation but also encompasses a wide array of techniques such as various 3DP methods and liquid-filled capsules, which will be detailed in the following text.

In this mini-review, we explore the various 3DP techniques employed for the direct fabrication of hybrid solid–liquid structures, such as extrusion,[8,27–36] material jetting[37–40] and vat photopolymerization (VP).[41,42] Techniques such as employing orthogonally

* *Correspondence to: EB Pentzer, Department of Chemistry, Texas A&M University, College Station, TX, 77843, USA. E-mail: emilypentzer@tamu.edu*

† *These authors contributed equally to this work.*

a *Department of Chemistry, Texas A&M University, College Station, TX, USA*

b *Department of Materials Science and Engineering, Texas A&M University, College Station, TX, USA*

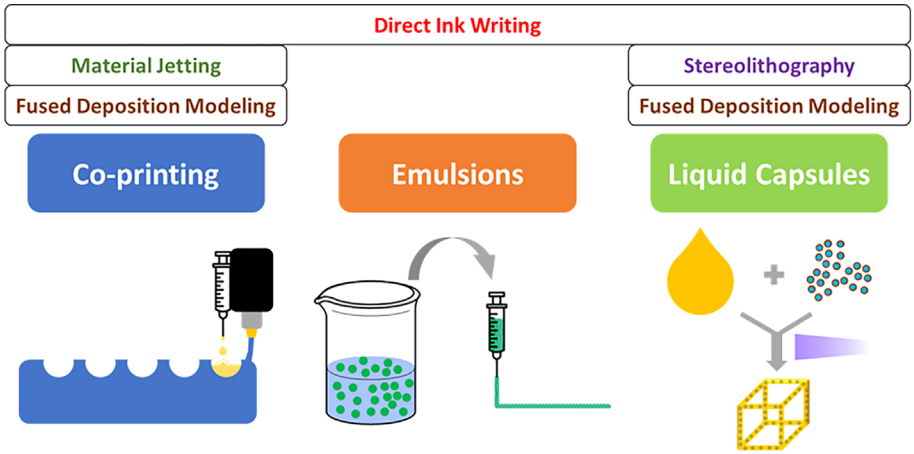

Figure 1. Summary of 3DP methods that have been employed to fabricate solid–liquid composites in the three major fabrication processes.

curable materials,[8,28–34,37–42] mid-print material changes,[28,33] multi-head printing,[8,27–42] emulsion-based inks[14–19,21,43–46] and integrating particle fillers[47–50] for single-feedstock printing and feedstock preparation are also presented and discussed. In general, three major categories, co-printing, emulsion-based inks and liquid-filled capsules, are identified (Fig. 1), and one miscellaneous section is also discussed. This mini-review focuses on liquids in ambient conditions and excludes, for example, solid–liquid phase change materials. Recently reviewed 3DP of pure LMs[51] and hydrogels[52] are not included either. The review concludes with a perspective on future directions, emphasizing the potential of bicontinuous interfacially jammed emulsion gels (bijels) in printing continuous liquid pathways and the importance of understanding ink formulation and stability. This insight into ongoing research brings us closer to realizing the manufacturing of custom SLCs tailored for specific applications.

METHOD 1: CO-PRINTING

The term 'co-printing' describes the simultaneous deposition of both solid and liquid components within a single structure, as coined by MacCurdy *et al*. in 2016.[39] An array of 3DP techniques have been used to co-print SLCs, including material jetting,[37–40] extrusion[8,27–36] and VP.[41,42] Extrusion-based methods, such as fused deposition modeling (FDM) and direct ink writing (DIW), typically allow only one nozzle to be active at a time, which generally limits print speed to a range of 800–2400 mm min^{-1}.[53] This approach also restricts resolution, with nozzle sizes setting bounds from 100 μm to 1 cm.[54] On the other hand, VP methods such as stereolithography (SLA), digital light processing and direct laser writing (DLW) have high resolutions, ranging from 0.1 to 100 μm, but are generally constrained by smaller build volumes.[54] The maximum build volume for extrusion-based printing can reach 100 × 100 × 100 cm^3, whereas that of VP techniques is slightly smaller (140 × 140 × 50 cm^3).[54] The build volume of DLW has not been explicitly documented; however, its emphasis on microscale and nanoscale fabrication implies smaller scales.[41,55] Additionally, switching materials during these processes to achieve multi-material prints is difficult. Therefore, harnessing either extrusion-based or VP for co-printing requires a combination with another technique, such as FDM paired with inkjet printing,[27,35] SLA paired with electrospraying,[42] DLW paired with vacuum filling[41] and DIW paired with microfluidics[28,33,34] and/or ultraviolet light curing.[8,28–34,37–42]

Co-printing: extrusion

Extrusion-based co-printing is the most widespread and primarily harnesses the modularity of these types of printers to combine multiple materials. One of the first examples of extrusion-based co-printing was reported in 2017 by Bastola *et al*.,[29] who printed a hybrid fluid-elastomeric magnetorheological material using a multi-material 3D printer equipped with extrusion-based time–pressure printheads (i.e. DIW with UV light). The authors printed a 30% v/v iron powder suspension in silicone grease shaped within a container, and then encapsulated each layer with a UV-curable elastomer resin. Further studies explored the influence of printing parameters[30] and geometries.[31,32] Through this co-printing method, printed parts exhibited improved damping capacity compared to conventional magnetorheological elastomers due to the incorporation of liquid fillers. Meanwhile, the fluid-containing composite could still be handled as solid despite the presence of the fluids in the solid matrix. However, the printing process relied on the shape of the magnetorheological fluid, set by the container used. As such, the geometric freedom of this approach was limited compared to other extrusion-based co-printing techniques. Mohammed and Kramer applied a similar method where elastomers were extruded at room temperature and LMs were spray-printed atop them to develop flexible and stretchable electronics.[8] Their four-step process—elastomer extrusion, LM slurry spray printing, mechanical sintering and final encapsulation—facilitates the creation of intricate conductive circuits and wearable devices. The adaptability of this process to integrate different materials underscores the evolving scope of extrusion-based co-printing in crafting advanced composite materials.

Li *et al*. developed an alternative co-printing approach by combining DIW with microfluidics and UV curing, enabling the printing of structures with controlled spatial distribution and composition of liquid inclusions.[33] Their ink consisted of two immiscible phases: a water–glycerol mixture and a commercial acrylate photopolymer resin. Using a microfluidic chip, they generated droplets of the water–glycerol mixture within the photopolymer resin, which were then extruded and cured by UV light. This method allowed for mid-print changes in the composition

of liquid inclusions and the incorporation of various compositions into a single part, demonstrating significant advancements in functional composite fabrication. Further, they replaced the aqueous phase with a two-part epoxy, which facilitated the self-healing of large cracks up to 500 μm in the printed structures. In a subsequent study, they incorporated silicone oil to enhance the impact resistance of photopolymer resin, resulting in co-printed structures with notably improved energy dissipation and impact resistance compared to pure resin.[34] In a similar vein, Wan and colleagues controlled the dispensation of droplet inclusions (Fig. 2(A)) to tune mechanical properties and endow magnetic responsivity to printed structures.[28] Specifically, they introduced aqueous polyethylene glycol diacrylate (PEGDA) droplets using microfluidics, which intrinsically softened the surrounding polydimethylsiloxane (PDMS) phase. Moreover, the inclusion of ferrofluid droplets enabled the creation of a magnetically responsive soft robotic actuator, which could lift and hold objects weighing several 100 mg. These works illustrate the potential of incorporating functional droplets to achieve desired mechanical and responsive properties in 3D-printed structures.

In the realm of co-printing, using multiple printheads for alternative dispensing of solid and liquid represents a significant advancement. In 2021, Youjun Hou filed for a patent on a multihead extrusion 3D printer capable of co-printing solid and liquid feedstocks.[36] The solid is printed from a filament, presumably a thermoplastic, and the liquid is deposited using a pneumatic nozzle. As the nozzles switch, the unused nozzle automatically retracts, eliminating the issue of nozzles dragging through deposited material. This approach was exemplified by Rupp and Binder, who developed a novel 3DP method using a dual-dispensing system for liquid and FDM (Fig. 2(B)),[27] which created core–shell capsule composites containing reactive liquids within a poly (ε-caprolactone) (PCL) matrix. Solid layers of PCL were printed, and then a PCL grid was printed atop to produce 100–800 μm voids. The voids were then filled with hydrophobic liquid from an inkjet dispenser and encapsulated with solid layers of PCL. Building upon this method, the authors printed a self-healing structure; the FDM feedstock consisted of solid nanocapsules that contained a trivalent azide and a dye and were mixed into PCL along with a catalyst, and the liquid component was a trivalent alkyne which was dispensed by inkjet. The authors later elaborated on this work by incorporating mechanophores in the PCL matrix to enable stress sensing within printed structures.[35] The ability to manufacture multicomponent specimens with separated reactive components while retaining post-printing activity underlines the importance of this work.

Co-printing: vat photopolymerization

There are limited studies utilizing VP for 3DP of hybrid solid–liquid structures. A notable work by Lee *et al*. combined SLA with electrospraying to fabricate porous scaffolds containing liquid-filled nanocapsules, targeting nerve regeneration applications.[42] The authors prepared capsules with diameters ranging from 80 to 327 nm by electrospraying with a core–shell needle where the core was an aqueous bovine serum albumin solution and the shell comprised poly(lactic-*co*-glycolic acid) in acetone. The photocrosslinkable hydrogel resin used for SLA consisted of poly(ethylene glycol) (PEG), PEGDA and a photoinitiator. Nanocapsules were incorporated into the resin by ultrasonication at concentrations of 0.1%, 0.5% and 1% w/v.

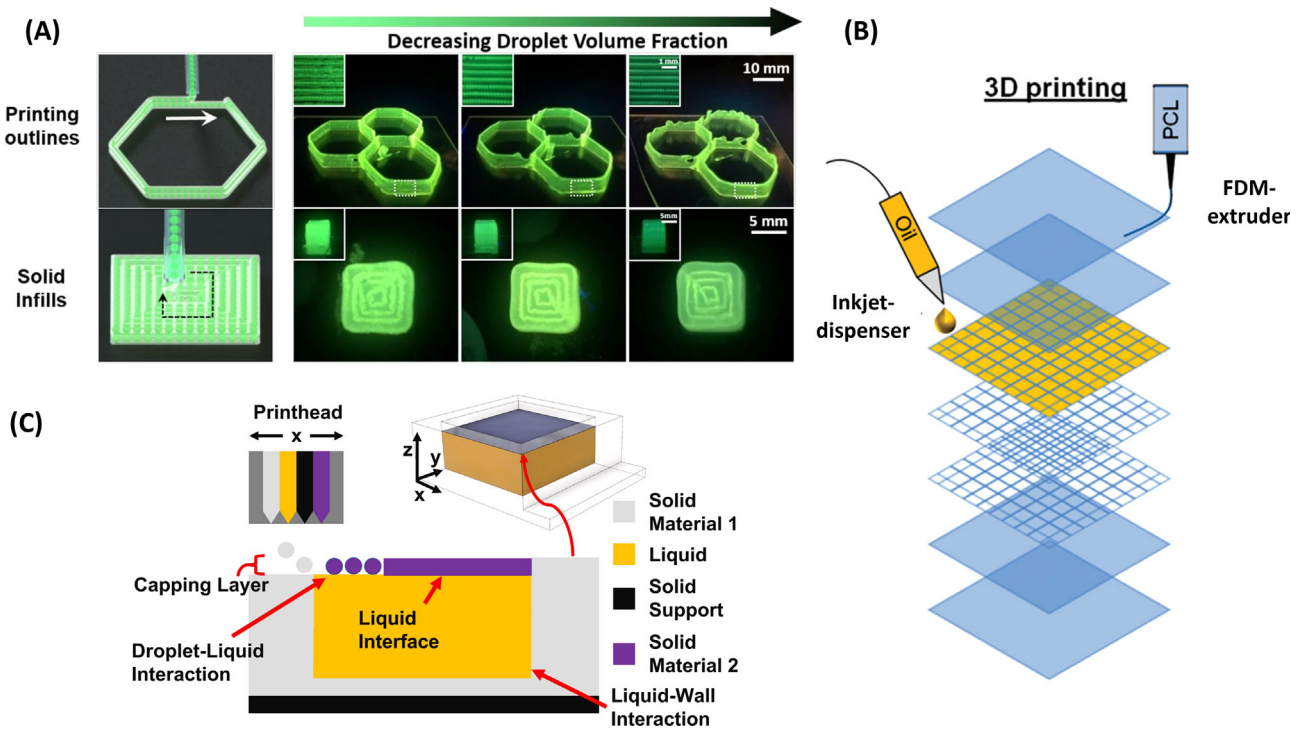

Figure 2. Overview of co-printing techniques. (A) Direct ink writing combined with microfluidics in which the liquid droplet volume was adjusted by the ratio of the flow rates of the two phases. Reproduced with permission from reference 28. Copyright 2020 The Proceedings of the National Academy of Sciences. (B) Fused deposition modeling (FDM) fabricating a solid substrate to encapsulate oil with an inkjet dispenser. Reproduced with permission from reference 27. Copyright 2020 Wiley-VCH. (C) Multi-material jetting using four nozzles to introduce different substances in a single object using the surface tension of the non-curable liquid to support the resins. Reproduced with permission from reference 37. Copyright 2022 Elsevier.

In another significant study, Acevedo *et al*. used DLW to print solid truncated spherical shells of 25 μm diameter from a photopolymer resin, leaving an opening atop each partial shell.[41] The vessels were vacuum-filled with water dyed with methylene blue, and then the capsules were sealed by printing a cap. This study presents an unprecedented method to modulate particle shape, wall thickness and size distribution for controlled containment and release of target liquids. Although VP techniques have been used to co-print hybrid solid–liquid structures, more than the printing methods are needed to be conducive to multi-material printing, and they are typically combined with other methods to overcome this limitation.

Co-printing: material jetting

In 2016, MacCurdy *et al*. reported a new method for printing multiple materials within the same part, including rigid and flexible solids, support material and liquid, to fabricate hydraulic robots in a single step.[39] The authors used an inkjet printer with four nozzles to deposit photopolymers with various properties and a non-curing liquid simultaneously to enable hydraulic operation. This process can simultaneously print solid and liquid materials, employing hydraulic channels to transmit force throughout the structure without manual assembly. It significantly simplifies robot fabrication and opens new design possibilities in robotics and automation. Building upon this work, the same group later used material jetting 3DP to deposit micro-scale droplets of acrylate-based photopolymer resin as a solidifying material and Stratasys model cleaning fluid as a non-solidifying material (Fig. 2(C)).[37] A vital aspect of this approach is leveraging the surface tension of the non-solidifying material to support the micro-droplets of photopolymer, which were deposited by the printer. Thus, the non-solidifying liquid can either be a support material removed from the structure after printing, or a working fluid that remains in the printed object to perform a desired function, which opens new horizons in the methodology of creating porous structures and SLCs. Lastly, the research by Bezek *et al*. significantly advanced 3DP with liquid inclusions, highlighting their impact on the mechanical and thermal properties of the printed objects.[38,40] Their findings demonstrate that even minor non-curing fluid inclusions can considerably alter properties like modulus and strength, which are vital for designing tissue-mimicking models in medical applications.

METHOD 2: EMULSION-BASED INKS

Emulsions are mixtures of at least two immiscible liquids, typically stabilized by a surfactant.[56] Achieving stable emulsions is sometimes challenging because it often involves factors such as salinity, temperature, pH, the dispersed phase ratio, the emulsifier/demulsifier concentration and the droplet size.[57] An equally crucial aspect is the selection of components that are compatible and non-reactive with each other. Emulsions can be harnessed as inks in 3DP, predominantly executed using DIW, and have found applications in producing porous structures,[58] the food industry,[14–19] biomedicine,[19,21] and energy transfer and storage.[43] Compared to the co-printing methods discussed above, emulsions can simplify the printer machinery because they necessitate only a single feedstock. However, the primary challenge is to ensure the inks have rheological properties ideal for DIW—shear-thinning, appropriate yield stress and thixotropy.[59] To achieve these desirable properties, several approaches have been explored. These include the use of high internal phase emulsions (HIPEs) (Fig. 3(A)),[16–19,44] particle jamming at liquid–liquid interfaces (Fig. 3(B)),[43] thickening the continuous phase (Fig. 3(C)),[14–16,18,21] droplet crosslinking (Fig. 3(D))[17,44] and LM droplets as fillers.[45,46] Notably, the stability and printability of emulsions are often enhanced through the synergistic combination of these strategies, ensuring an effective ink formulation.

HIPEs, with a discontinuous phase volume >74%,[60] can be effectively utilized as inks in DIW, provided appropriate compositions are realized.[59] A prime example is the work of Song and colleagues, who employed DIW to 3D print corn-oil-in-water HIPEs stabilized by cellulose nanocrystals (CNCs) (Fig. 3(A)).[19] They extensively investigated the effect of pH and ionic strength on the HIPE formation and 3D printability, identifying optimal conditions (pH 5–8 and 25–200 mmol L^{-1} NaCl) for producing HIPEs. These inks were then 3D printed by DIW with high resolution and fidelity.

The viscoelasticity essential for DIW inks can also be achieved by interfacial jamming of nanomaterials, as exemplified by Xing and colleagues.[43] They introduced a viscoelastic Pickering emulsion gel (emulgel) amenable to DIW printing. Notably, this research demonstrated post-print solidification through crosslinking, showcasing the advanced integration of materials like liquid paraffin, sulfur in CS_2 solution or paraffin wax into the printing process (Fig. 3(B)). The emulgel derives its stability and viscoelastic properties from jammed graphene oxide (GO) nanosheets and the coagent didodecyldimethylammonium bromide (DDAB). Importantly, the printed structures undergo crosslinking with ethylenediamine, and exposure to hydrazine hydrate vapor chemically reduces the nanosheets to impart thermal and electrical conductivity. A notable feature is the high sulfur loading of up to 90% in the printed objects. Furthermore, carboxylate-modified carbon nanotubes can be incorporated without affecting the emulgel stability, paving the way for printed energy storage and conversion devices, such as supercapacitors and Li–S batteries, demonstrating the versatility of the system without compromising emulgel stability.

Thickening of the continuous phase can be an alternative to the methods mentioned above, and supramolecular interactions are useful in this approach due to their reversible nature. Shahbazi, Jäger and their team used acetylated microcrystalline cellulose (AMCC) as a surfactant and thickener, forming hydrogen bonds with casein.[14,15] Similarly, Rojas, Filonenko and colleagues employed PEG and α-cyclodextrin to form a supramolecular host–guest hydrogel in the continuous phase of a CNC-stabilized emulsion.[21] This innovation imparted the rheological properties required for DIW, providing a storage modulus up to *ca* 113 kPa and shear-thinning behavior, facilitating the 3DP of complex structures with high fidelity and structural integrity (Fig. 3(C)).[21] The exclusion of a small molecule coagent, which is frequently employed for such systems, reduced the complexity and enhanced the biocompatibility of the system. Notably, this approach led to printed objects that exhibited only slight dimensional shrinkage (*ca* 7%) post-freeze-drying, indicating excellent structural retention. This method's potential extends to designing biocompatible inks for applications in food, pharmaceuticals and biomedical devices. Although HIPEs are often printable independently, thickening agents may be employed to enhance printability.[16,18] Xu and colleagues developed flavor oil-in-water HIPEs with casein/pectin hybrid particles.[16] In this system, the pectin served as a thickening agent, stabilizing HIPE-based inks by forming hydrogen bonds with amide groups in casein. This study demonstrated that the viscosity and gel strength of HIPEs improved

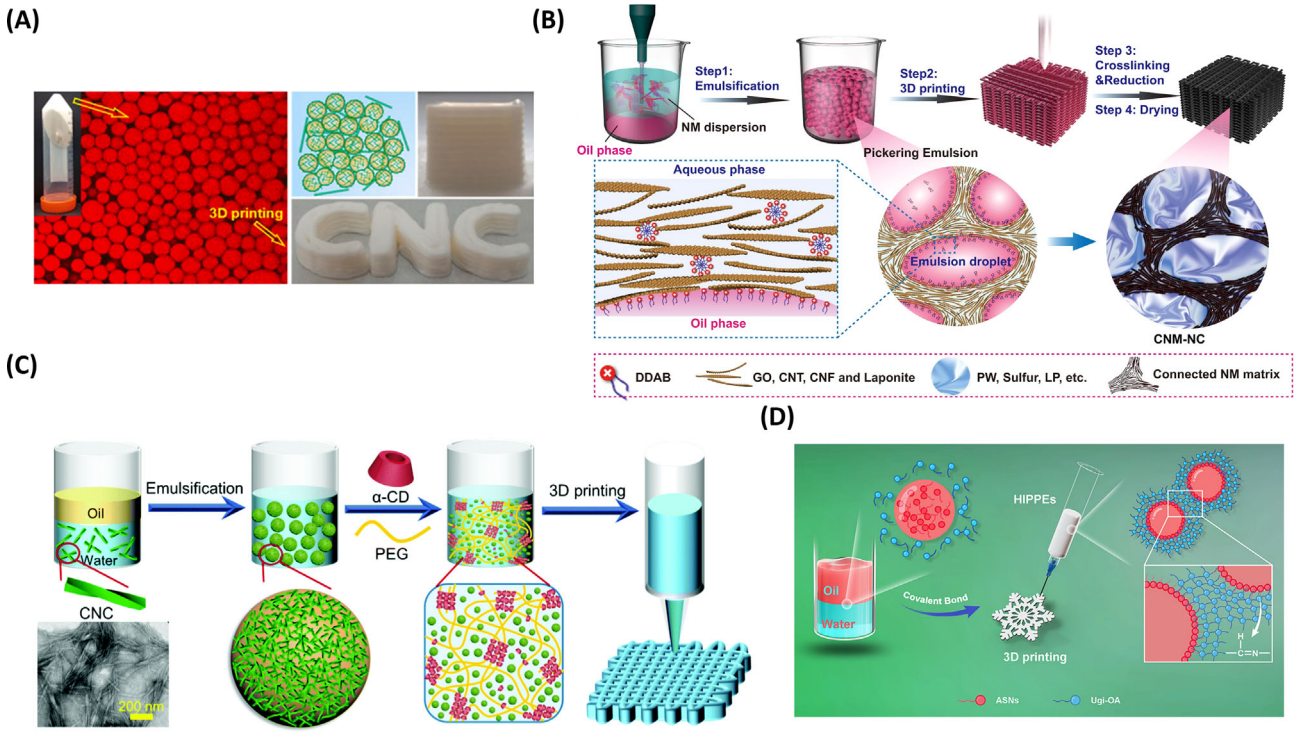

Figure 3. Stabilization techniques for emulsion-based inks for direct ink writing. (A) Paste-like high internal phase emulsions (HIPEs) stabilized by cellulose nanocrystals. Reproduced with permission from reference 19. Copyright 2022 Elsevier. (B) Graphene oxide (GO) particles jamming at interfaces of stabilized emulsion droplets. Reproduced with permission from reference 43. Copyright 2021 CC-BY-NC-ND. (C) Thickening of the continuous phase using a supramolecular host–guest hydrogel. Reproduced with permission from reference 21. Copyright 2022 CC-BY-NC-ND. (D) Droplets crosslinked by interfacial coassembly of aldehyde-modified alginate polysaccharides (Ugi-OA) and aminated silica nanoparticles (ASNs). Reproduced with permission from reference 44. Copyright 2023 American Chemical Society.

with increasing pectin concentration, facilitating stable 3DP with enhanced shape retention. Conversely, dynamic covalent chemistry was employed by Feng *et al*. with a pea protein isolate-high methoxyl pectin-epigallocatechin gallate (PPI-HMP-EGCG) complex as the surfactant and thickener.[18] The complex augmented the stability and viscosity of the Pickering HIPEs containing tea camellia seed oil and cinnamaldehyde, creating suitable rheological properties for 3DP. Notably, the complex facilitated the Schiff base reaction between cinnamaldehyde and protein amino groups, enhancing protein adsorption on the droplets to form a compact layer. The authors successfully printed various HIPE structures with minimal loss (*ca* 11%) of cinnamaldehyde during printing, a significant achievement in liquid retention in 3D-printed SLCs.

Droplet crosslinking is a crucial supplementary method alongside HIPEs to bolster droplet–droplet interactions.[17,44] Xu and colleagues reported HIPEs stabilized by cod proteins, where covalent disulfide linkages were formed between droplets, enhancing the printability and extrudability of the HIPEs.[17] This process leveraged the concentration-dependent cod protein crosslinking networks within the HIPEs, significantly increasing their stability, gel strength and viscosity. The resulting HIPEs exhibited remarkable long-term stability and excellent printability. Complementing this, Li and colleagues employed the Schiff base interaction to stabilize HIPEs (Fig. 3(D)).[44] They utilized aldehyde-modified alginate polysaccharides (Ugi-OA) and aminated silica nanoparticles (ASNs) to form interfacial assemblies that stabilized the biphasic system. This approach resulted in thicker and more rigid interfacial films than the non-aminated silica nanoparticles. Their work underscores that microscopic changes in interfacial morphology due to Schiff base interaction significantly influence the macroscopic properties of HIPEs. Their findings bridge the gap between colloidal interface science and soft materials technology, offering insights into the stabilization mechanisms of HIPEs and 3DP.

The eutectic alloy of gallium and indium (EGaIn) (75.5 wt% Ga and 24.5 wt% In) is known for its 3D printability, attributed to the formation of an oxide layer upon extrusion in air.[45,46,51,61–63] This property allows EGaIn to retain its structure in the continuous phase without requiring surfactants, which are typically essential in emulsion systems.[3] However, additional encapsulation is still needed to prevent liquid leakage and handling damage. Dickey and colleagues presented a novel approach to address this and produced a self-encapsulating LM–silicone dispersion using DIW.[45] Their approach utilized high loadings of LM in silicone, enhancing the viscosity of the silicone and producing a gel-like substance suitable for DIW. This technique facilitated the formation of metal-rich interior conductive layers and insulating exterior layers, circumventing the need for further encapsulation. This dual-layer composition is particularly advantageous in soft electronics and wearable technologies, providing necessary insulation and conductivity in one structure. Complementing this, Haake *et al*. developed a novel 3DP technique for creating LM–composite microstructures.[46] This method uniquely allows *in situ* control of the microstructure shape, orientation and connectivity within elastomer composites. Unlike traditional inks with rigid particles, emulsion inks with LM fillers enable dynamic microstructural programming. The printed materials are soft, highly deformable, and can be made conductive or insulating by altering

process conditions. This technique enables materials with varying local properties and presents novel opportunities for designing multifunctional soft materials.

Although the aforementioned papers display an array of emulsion-based printing approaches, many of these reports do not address curing or solidification. As a result, the final prints were much softer than those prepared by co-printing. This softness aligns with requirements in the food and biomedical sectors, where material flexibility and texture are crucial. However, further research into curable matrices is essential to enhance the structural integrity and expand the applicability of these emulsion-based feedstocks in various industrial applications.

METHOD 3: LIQUID-FILLED CAPSULES

Compared to the previous two methods, using liquid-filled capsules as additives is relatively less studied. This approach requires minimal adjustments to the printing setup and more straightforward feedstock preparation, in contrast to the more complex co-printing methods that demand specialized setups and emulsion-templating which involves intricate interactions among multiple components. The preparation only involves simple mixing of traditional feedstocks and capsules,[47–50] which can streamline the 3DP of SLCs.

The Chin group innovated an SLC comprising a commercial thermoset photopolymer resin and capsules filled with anisole and poly(methyl methacrylate) (PMMA) using SLA.[50] They embedded microcapsules prepared via an emulsion-templated *in situ* polymerization of urea-formaldehyde into the UV-curable resin. Surprisingly, no adverse effects on print quality were caused by light scattering. Upon rupture, the microcapsules released the PMMA and anisole to 'solvent weld' and heal the structure. After this self-healing at 25 °C for 3 days, the sample recovered 87% of its initial critical toughness. Likewise, Beckingham and colleagues enhanced the mechanical properties and sustainability of thermosets in SLA by incorporating double-walled polyurethane/poly(urea-formaldehyde) microcapsules containing dicyclopentadiene into a commercial resin with Grubbs catalyst (Fig. 4(A)).[47] This led to a healing efficiency of 73% at room temperature.

Diverging from previous studies, the Beckingham group also demonstrated solvent-based self-healing of thermoplastic composites using FDM (Fig. 4(B)).[48] They prepared and embedded double-walled microcapsules containing ethyl phenylacetate (EPA) into a tetrahydrofuran solution of high-impact polystyrene (HIPS). This solution was used to coat an HIPS filament using a continuous bath coater for 3DP. Post-print evaluation by ^{1}H NMR spectroscopy and TGA indicated that the capsules survived

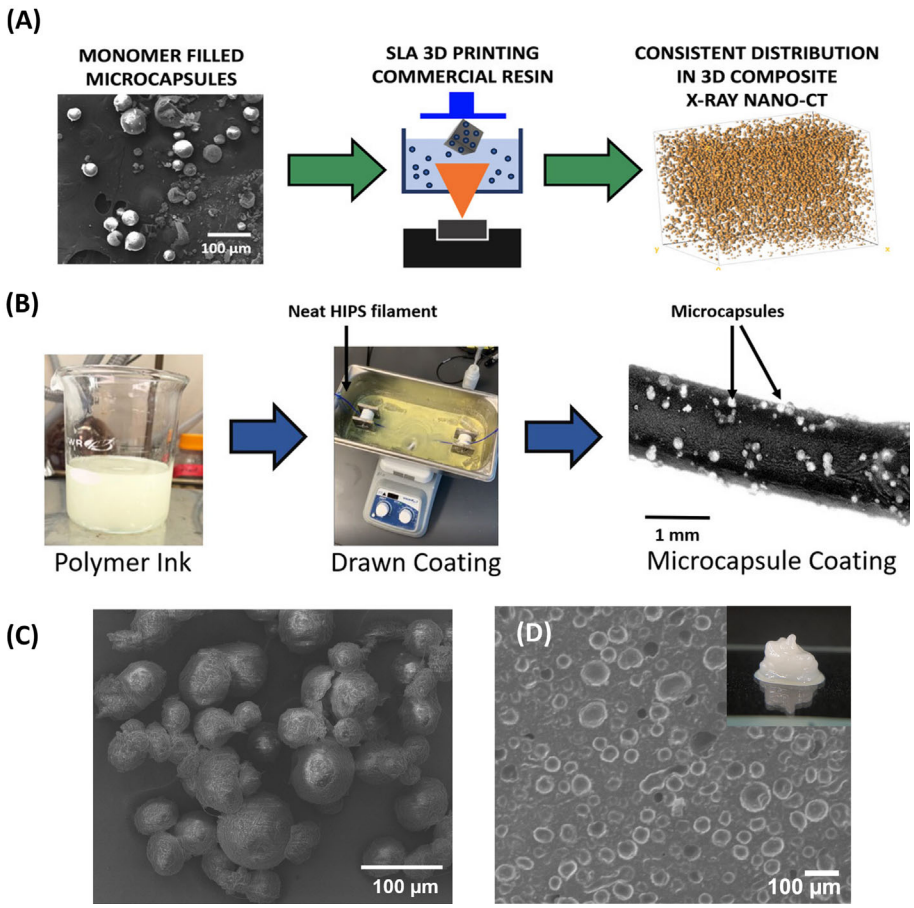

Figure 4. Liquid-filled capsules in 3DP feedstocks. (A) Stereolithography (SLA) feedstock prepared by dispersing microcapsules in commercial resin. Reproduced with permission from reference 47. Copyright 2020 American Chemical Society. (B) Preparation of fused deposition modeling (FDM) filaments coated with capsules by drawn coating. Reproduced with permission from reference 48. Copyright 2022 American Chemical Society. (C) SEM images of capsules prepared by interfacial polymerization. (D) Cross-sectional SEM image of printed ink containing capsules in a polymer matrix (inset shows the uncured ink). Reproduced with permission from reference 49. Copyright 2022 The Royal Society of Chemistry.

the coating, heating and extrusion-based printing. When printed samples were damaged by impact, the capsules ruptured and the EPA was released to the damaged site, promoting chain mobility and healing cracked surfaces. A fracture toughness recovery of up to 81% was observed in single-edge notch beam testing.

The work by our laboratory contrasts with these approaches. Cipriani *et al*. utilized a modular platform in DIW to fabricate a liquid–solid monolith with a single feedstock ink.[49] The capsules had a core of industrial lubricant poly(α-olefin)$_{432}$ (PAO_{432}) and a shell of carbon particles and polyurea (Fig. 4(C)) as rheological modifiers, which endowed shear-thinning and thixotropy to either commercially available thermoplastic polyurethane (TPU) dissolved in *N*,*N*-dimethylformamide or a photocurable resin. The composite inks could be cured by solvent removal or UV-crosslinking, respectively, to give polymeric monoliths containing pockets of PAO_{432} liquid (Fig. 4(D)). In this work, polymer matrices were not limited to photocurable resin, and printing could be performed at room temperature, indicating compatibility with capsules containing volatile components. Of note, structures printed from the TPU-based ink leaked oil over time, which we hypothesized was due to the presence of small pores formed upon solvent removal. Thus, modifying the polymer matrix allows one to achieve the desired functionality, such as controlled delivery of target liquids.

Although mixing liquid-filled capsules with matrix feedstocks seems straightforward and modular, the capsules must be sufficiently robust to resist rupture during printing, and they must also be compatible with the matrices to avoid phase separation. Moreover, future applications other than self-healing should be investigated and proposed.

METHOD 4: MISCELLANEOUS

While the three primary methods discussed earlier are the most widely used approaches to printing SLCs, recent advancements expand beyond these categories. Examples include leveraging high surface area vacuum absorbents,[64] LM deposition with laser sintering[65] and phase separation techniques.[66,67] The following is a summary of these related studies.

The Kim group fabricated a library of lubricant–polymer composites by combining liquid polymer resin with silica aerogel particles dispersed in an oil lubricant to form a 3D-lubric platform. This innovative approach employed various combinations of resin (perfluoropolyether, silicone elastomer or poly(lactic acid)) and oil lubricants (silicone oil, mineral oil or olive oil) (Fig. 5(A)).[64] The silica aerogel particles enhanced the compatibility between the lubricant and polymer, lending the rheological properties necessary for 3DP and mitigating swelling. This platform was used to fabricate UV-curable or thermally curable self-cleaning containers and antibacterial/bactericidal medical tubes, showcasing suppressed mass losses of encapsulated oils (<5%) compared to oil-infused silicone (about 15%). While long-term stability and biocompatibility remain to be reported, this technique offers a promising direction in encapsulating oils with controlled release properties.

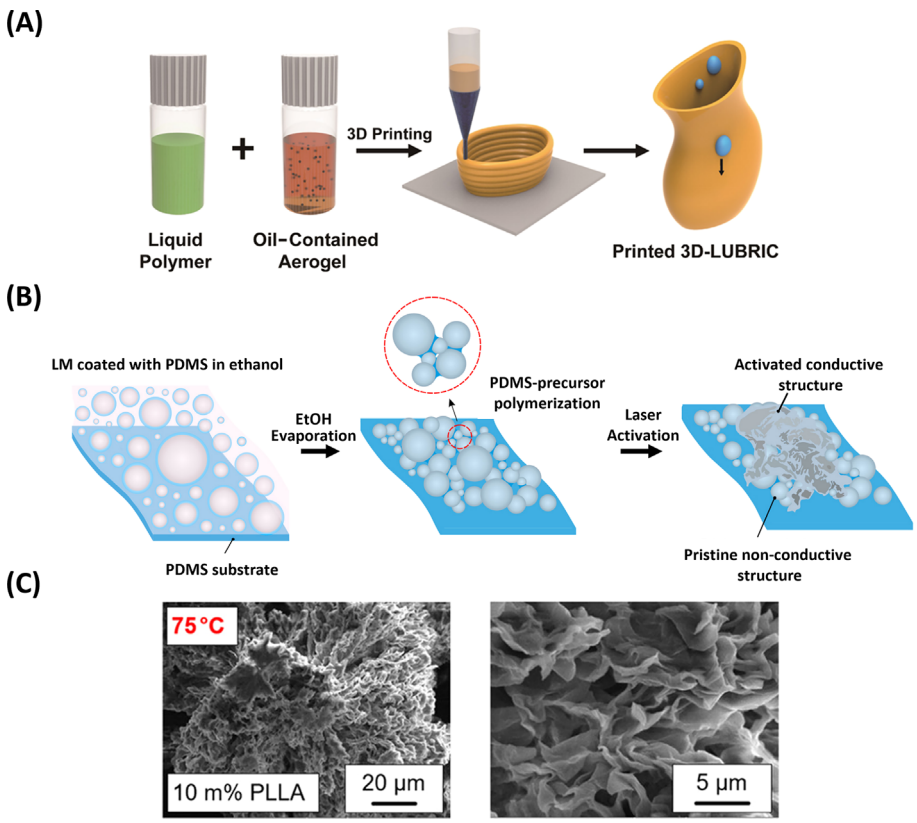

Figure 5. Additional approaches to printing solid–liquid composites. (A) Porous silica aerogel particles were employed to prevent phase separation in the direct ink writing ink. Reproduced with permission from reference 64. Copyright 2020 American Chemical Society. (B) Direct laser writing of a double emulsion containing liquid metals (LMs) and polydimethylsiloxane (PDMS) precursor. Reproduced with permission from reference 65. Copyright 2021 American Chemical Society. (C) SEM images of the microporous scaffold formed from solid–liquid phase separation of poly(L-lactic acid) (PLLA) and IR3535. Reproduced with permission from reference 66. Copyright 2021 American Chemical Society.

In contrast to the LM droplet fillers, Kramer-Bottiglio and coauthors prepared an LM (EGaIn) and PDMS composite using a double emulsion template, serving as a DLW ink (Fig. 5(B)).[65] This composition involved EGaIn-in-ethanol emulsions and PDMS precursors, where the ethanol was evaporated and the droplets were laser sintered, forming electrically conductive pathways once printed. Although a double emulsion was present in the system, this method was not categorized as emulsion-templating because the continuous phase (ethanol) was removed before printing. This scalable and facile method could produce samples with high conductivity due to their uniform and continuous morphology. The printed circuits maintained stable electrical and mechanical performance under various strains, including twisting, bending and stretching to 80% strain and repeated stretching and releasing to 50% strain for 100 cycles.

It was discussed in the introduction that solid–liquid phase separation can also be used to prepare SLCs, and Androsch and colleagues further combined the phase separation with 3DP.[66,67] They created a polymer/liquid insect repellent system based on the phase separation of PLLA and ethyl butylacetylaminopropionate (IR3535), which was 3D printed into payload delivery devices. The feedstock was prepared by solution mixing, and a solid scaffold hosting the liquid repellent was formed via crystallization-based solid–liquid thermally induced phase separation (Fig. 5(C)). The resultant printed wearable devices effectively released the repellent for 5–10 days, maintaining functionality and demonstrating a maximum loading of 25% by mass.

PERSPECTIVE

3DP methods of SLCs (Fig. 1) complement the more traditional approach of printing porous structures and then backfilling with liquids.[68] Although the single-step direct method has many merits, practical implementation is currently limited due to several challenges. For example, although relatively well studied, co-printing multiple feedstocks requires hardware modification to extrude from multiple dispensers. That can become costly and complicated, requiring process optimization for each feedstock composition. Further, material waste can also be an issue if the setup is not optimized. Emulsion-based inks are attractive because they are cost-effective. Nevertheless, the interplay between the continuous phase, dispersed phase, surfactants, rheology modifiers, concentration, pH and temperature can be challenging, again requiring optimization for each desired composition or application. The stability of emulsions and printed objects is important, as emulsion destabilization or phase separation may occur. Also, these systems often generate soft products unsuitable for all end-use applications unless post-curing is applied. At present, while the majority of emulsion 3DP focuses on HIPEs, bicontinuous jammed emulsion gels (bijels) or those with a unique tortuous bicontinuous microstructure are emergent candidates for feedstocks due to the unique interconnectivity of the two phases and potentially beneficial rheological properties. However, only a few studies have been reported.[69,70] The spattering of miscellaneous methods used to produce SLCs also provides a platform to understand alternative methods and their challenges better. For example, the propensity of LM to settle in polymer matrices and phase separation dynamics between liquid and solid components must be further examined to broaden the applications of 3D-printed hybrid solid–liquid structures.

One of the most modular approaches to printing SLCs is using liquid-filled capsules. This platform is bolstered by the many modular approaches to prepare capsules with diverse core materials, including microfluidics,[71] hard templating[72] and soft templating.[73] Off-the-shelf printing methods, especially DIW, enable printing without complex infrastructure. The major challenges to this approach are the compatibility of the capsules and the matrices (so that they do not phase separate, and the capsule liquid is not removed) and the mechanical strength of the capsules (as they should not rupture upon printing/extrusion). Of note, for light-based curing of inks, concerns may also arise if capsules scatter or absorb the wavelength required for photopolymerization. As a result, the influence of capsule properties (e.g. sizes, hardness, wettability and compatibility with the matrices) on necessary printing parameters is worth exploring to facilitate future distributed printing. This can be bolstered by robust and replicable materials preparation and printing methods.

On top of the methods mentioned above, 3DP of SLCs through lamination and powder-bed fusion has yet to be reported. Lamination is challenging for preparing SLCs because the process requires feedstock in sheets,[74,75] while liquids do not have a fixed shape. On the other hand, powder-bed fusion seems more promising, and there have been a few reports on selective laser sintering (SLS) of non-pristine polymers (e.g. those with electrically conductive coatings).[76–78] Hence, core–shell liquid–solid capsules are intriguing feedstocks for SLS. In achieving SLS printing, accurate control of the laser power and heating bed during sintering, the surface tension of the melted polymers, volatility, flammability of the liquids, and the interactions between the solid and liquid should all be considered.

Hybrid solid–liquid 3D prints offer tailorable compositions, custom geometries and unique properties integral to advancements across various fields. This burgeoning area of research has the potential to advance a fundamental understanding of print processes and dramatically expand the types of functional composite materials that can be accessed. The future of hybrid solid–liquid 3DP is promising and is particularly anticipated to revolutionize fields such as bio-based materials,[79,80] responsive materials[81,82] and drug delivery systems.[82] Future collaboration between materials scientists, polymer chemists, 3DP experts, characterization specialists and end users will open doors to new techniques and cutting-edge applications.

ACKNOWLEDGEMENTS

This work was funded by NSF DMR (Grant no. 2103182) and Texas A&M University. C.E.C. is supported by a NASA Space Technology Graduate Research Opportunity. The authors appreciate Dr Peiran Wei for his valuable suggestions on the manuscript structure.

REFERENCES

1 Bartlett MD and Style RW, *Soft Matter* **16**:5799–5800 (2020). https://doi.org/10.1039/D0SM90113J.
2 Barron EJ III, Williams ET, Tutika R, Lazarus N and Bartlett MD, *RSC Appl Polym* **1**:315–324 (2023). https://doi.org/10.1039/D3LP00109A.
3 Style RW, Tutika R, Kim JY and Bartlett MD, *Adv Funct Mater* **31**:2005804 (2021). https://doi.org/10.1002/adfm.202005804.
4 Deng F, Nguyen Q-K and Zhang P, *Addit Manuf* **33**:101117 (2020). https://doi.org/10.1016/j.addma.2020.101117.
5 Markvicka EJ, Bartlett MD, Huang X and Majidi C, *Nat Mater* **17**:618–624 (2018). https://doi.org/10.1038/s41563-018-0084-7.
6 Barron EJ III, Williams ET, Wilcox BT, Ho DH and Bartlett MD, *J Polym Sci* **1**:1–12 (2023). https://doi.org/10.1002/pol.20230616.
7 Tutika R, Haque ABMT and Bartlett MD, *Commun Mater* **2**:64–68 (2021). https://doi.org/10.1038/s43246-021-00169-4.

8 Mohammed MG and Kramer R, *Adv Mater* **29**:1604965 (2017). https://doi.org/10.1002/adma.201604965.
9 Zhang Y-F, Zhang N, Hingorani H, Ding N, Wang D, Yuan C *et al.*, *Adv Funct Mater* **29**:1806698 (2019). https://doi.org/10.1002/adfm.201806698.
10 Majidi C, Alizadeh K, Ohm Y, Silva A and Tavakoli M, *Flex Print Electron* **7**:013002 (2022). https://doi.org/10.1088/2058-8585/ac515a.
11 Zhu L, Wang B, Handschuh-Wang S and Zhou X, *Small* **16**:1903841 (2020). https://doi.org/10.1002/smll.201903841.
12 Zhou W, Dou M, Timilsina SS, Xu F and Li X, *Lab Chip* **21**:2658–2683 (2021). https://doi.org/10.1039/D1LC00414J.
13 Wang J, Li Y, Gao Y, Xie Z, Zhou M, He Y *et al.*, *Ind Crops Prod* **112**:281–289 (2018). https://doi.org/10.1016/j.indcrop.2017.12.022.
14 Shahbazi M, Jäger H and Ettelaie R, *Colloids Surf A Physicochem Eng Asp* **622**:126641 (2021). https://doi.org/10.1016/j.colsurfa.2021.126641.
15 Shahbazi M, Jäger H and Ettelaie R, *Colloids Surf A Physicochem Eng Asp* **624**:126760 (2021). https://doi.org/10.1016/j.colsurfa.2021.126760.
16 Bi A-Q, Xu X-B, Guo Y, Du M, Yu C-P and Wu C, *Food Chem* **371**:131349 (2022). https://doi.org/10.1016/j.foodchem.2021.131349.
17 Li X, Xu X, Song L, Bi A, Wu C, Ma Y *et al.*, *ACS Appl Mater Interfaces* **12**:45493–45503 (2020). https://doi.org/10.1021/acsami.0c11434.
18 Feng T, Fan C, Wang X, Wang X, Xia S and Huang Q, *Food Hydrocoll* **124**:107265 (2022). https://doi.org/10.1016/j.foodhyd.2021.107265.
19 Ma T, Cui R, Lu S, Hu X, Xu B, Song Y *et al.*, *Food Hydrocoll* **125**:107418 (2022). https://doi.org/10.1016/j.foodhyd.2021.107418.
20 Atinafu DG, Kim YU, Kim S, Kang Y and Kim S, *Small* **20**:2305418 (2023). https://doi.org/10.1002/smll.202305418.
21 Pang B, Ajdary R, Antonietti M, Rojas O and Filonenko S, *Mater Horiz* **9**:835–840 (2022). https://doi.org/10.1039/D1MH01741A.
22 Tutika R, Kmiec S, Haque ABMT, Martin SW and Bartlett MD, *ACS Appl Mater Interfaces* **11**:17873–17883 (2019). https://doi.org/10.1021/acsami.9b04569.
23 Style RW, Sai T, Fanelli N, Ijavi M, Smith-Mannschott K, Xu Q *et al.*, *Phys Rev X* **8**:011028 (2018). https://doi.org/10.1103/PhysRevX.8.011028.
24 Watson AM, Cook AB and Tabor CE, *Adv Eng Mater* **21**:1900397 (2019). https://doi.org/10.1002/adem.201900397.
25 Klein TR, Kirillova A, Gall K and Becker ML, *RSC Appl Polym* **1**:73–81 (2023). https://doi.org/10.1039/D3LP00013C.
26 Cipriani CE, Dornbusch DA, Vivod SL and Pentzer EB, *RSC Appl Polym* **2**:71–86 (2024). https://doi.org/10.1039/D3LP00200D.
27 Rupp H and Binder WH, *Adv Mater Technol* **5**:2000509 (2020). https://doi.org/10.1002/admt.202000509.
28 Mea HJ, Delgadillo L and Wan J, *Proc Natl Acad Sci* **117**:14790–14797 (2020). https://doi.org/10.1073/pnas.1917289117.
29 Bastola AK, Hoang VT and Li L, *Mater Des* **114**:391–397 (2017). https://doi.org/10.1016/j.matdes.2016.11.006.
30 Bastola AK, Paudel M and Li L, *Polymer* **149**:213–228 (2018). https://doi.org/10.1016/j.polymer.2018.06.076.
31 Bastola AK, Paudel M and Li L, *J Magn Magn Mater* **494**:165825 (2020). https://doi.org/10.1016/j.jmmm.2019.165825.
32 Bastola A, Paudel M and Li L, *J Intell Mater Syst Struct* **31**:377–388 (2020). https://doi.org/10.1177/1045389X19891557.
33 Li X, Zhang JM, Yi X, Huang Z, Lv P and Duan H, *Adv Sci* **6**:1800730 (2019). https://doi.org/10.1002/advs.201800730.
34 Yu M, Li X, Lv P and Duan H, *Acta Mech Solida Sin* **34**:911–921 (2021). https://doi.org/10.1007/s10338-021-00277-1.
35 Rupp H and Binder WH, *Macromol Rapid Commun* **42**:2000450 (2021). https://doi.org/10.1002/marc.202000450.
36 Hou Y, Solid–liquid-material combined double-headed 3D printer and printing method, WO patent 2021031444A1 (2021).
37 Hayes B, Hainsworth T and MacCurdy R, *Addit Manuf* **55**:102785 (2022). https://doi.org/10.1016/j.addma.2022.102785.
38 Bezek LB, Chatham CA, Dillard DA and Williams CB, *J Mech Behav Biomed Mater* **125**:104938 (2022). https://doi.org/10.1016/j.jmbbm.2021.104938.
39 MacCurdy R, Katzschmann R, Kim Y and Rus D, *2016 IEEE International Conference on Robotics and Automation (ICRA)* 3878–3885 (IEEE, 2016) https://doi.org/10.1109/ICRA.2016.7487576.
40 Bezek LB, Cauchi MP, Vita RD, Foerst JR and Williams CB, *J Mech Behav Biomed Mater* **110**:103971 (2020). https://doi.org/10.1016/j.jmbbm.2020.103971.
41 Acevedo R, Restaino MA, Yu D, Hoag SW, Flank S and Sochol RD, *J Microelectromechanical Syst* **29**:924–929 (2020). https://doi.org/10.1109/JMEMS.2020.3000479.
42 Lee S-J, Zhu W, Heyburn L, Nowicki M, Harris B and Zhang LG, *IEEE Trans Biomed Eng* **64**:408–418 (2017). https://doi.org/10.1109/TBME.2016.2558493.
43 Zhang Y, Zhu G, Dong B, Wang F, Tang J, Stadler FJ *et al.*, *Nat Commun* **12**:111 (2021). https://doi.org/10.1038/s41467-020-20299-6.
44 Wang Z, Huang S, Zhao X, Yang S, Mai K, Qin W *et al.*, *ACS Appl Mater Interfaces* **15**:23989–24002 (2023). https://doi.org/10.1021/acsami.3c03642.
45 Neumann TV, Facchine EG, Leonardo B, Khan S and Dickey MD, *Soft Matter* **16**:6608–6618 (2020). https://doi.org/10.1039/D0SM00803F.
46 Haake A, Tutika R, Schloer GM, Bartlett MD and Markvicka EJ, *Adv Mater* **34**:2200182 (2022). https://doi.org/10.1002/adma.202200182.
47 Shinde VV, Celestine A-D, Beckingham LE and Beckingham BS, *ACS Appl Polym Mater* **2**:5048–5057 (2020). https://doi.org/10.1021/acsapm.0c00872.
48 Shinde VV, Taylor G, Celestine ADN and Beckingham BS, *ACS Appl Polym Mater* **4**:3324–3332 (2022). https://doi.org/10.1021/acsapm.1c01884.
49 Cipriani CE, Starvaggi NC, Edgehouse KJ, Price JB, Vivod SL and Pentzer EB, *Mol Syst Eng* **7**:1039–1044 (2022). https://doi.org/10.1039/D2ME00102K.
50 Sanders P, Young AJ, Qin Y, Fancey KS, Reithofer MR, Guillet-Nicolas R *et al.*, *Sci Rep* **9**:388 (2019). https://doi.org/10.1038/s41598-018-36828-9.
51 Zou Z, Chen Y, Yuan S, Luo N, Li J and He Y, *Adv Funct Mater* **33**:2213312 (2023). https://doi.org/10.1002/adfm.202213312.
52 Kaliaraj GS, Shanmugam DK, Dasan A and Mosas KKA, *Gels* **9**:260 (2023). https://doi.org/10.3390/gels9030260.
53 Theagarajan R, Moses JA and Anandharamakrishnan C, *Food Bioproc Tech* **13**:1048–1062 (2020). https://doi.org/10.1007/s11947-020-02453-6.
54 Daminabo SC, Goel S, Grammatikos SA, Nezhad HY and Thakur VK, *Mater Today Chem* **16**:100248 (2020). https://doi.org/10.1016/j.mtchem.2020.100248.
55 Nishiyama H, Umetsu K and Kimura K, *Sci Rep* **9**:14310 (2019). https://doi.org/10.1038/s41598-019-50630-1.
56 Wei P, Luo Q, Edgehouse KJ, Hemmingsen CM, Rodier BJ and Pentzer EB, *ACS Appl Mater Interfaces* **10**:21765–21781 (2018). https://doi.org/10.1021/acsami.8b07178.
57 Zolfaghari R, Fakhru'l-Razi A, Abdullah LC, Elnashaie SS and Pendashteh A, *Sep Purif Technol* **170**:377–407 (2016). https://doi.org/10.1016/j.seppur.2016.06.026.
58 Liu Q and Zhai W, *ACS Appl Mater Interfaces* **14**:32196–32205 (2022). https://doi.org/10.1021/acsami.2c03245.
59 Wei P, Cipriani C, Hsieh C-M, Kamani K, Rogers S and Pentzer E, *J Appl Phys* **134**:100701 (2023). https://doi.org/10.1063/5.0155896.
60 Pulko I and Krajnc P, *Macromol Rapid Commun* **33**:1731–1746 (2012). https://doi.org/10.1002/marc.201200393.
61 Xu Q, Oudalov N, Guo Q, Jaeger HM and Brown E, *Phys Fluids* **24**:063101 (2012). https://doi.org/10.1063/1.4724313.
62 Jacob AR, Parekh DP, Dickey MD and Hsiao LC, *Langmuir* **35**:11774–11783 (2019). https://doi.org/10.1021/acs.langmuir.9b01821.
63 Elton ES, Reeve TC, Thornley LE, Joshipura ID, Paul PH, Pascall AJ *et al.*, *J Rheol* **64**:119–128 (2020). https://doi.org/10.1122/1.5117144.
64 Ahn J, Jeon Y, Lee KW, Yi J, Kim SW and Kim DR, *ACS Appl Mater Interfaces* **12**:26464–26475 (2020). https://doi.org/10.1021/acsami.0c05764.
65 Liu S, Kim SY, Henry KE, Shah DS and Kramer-Bottiglio R, *ACS Appl Mater Interfaces* **13**:28729–28736 (2021). https://doi.org/10.1021/acsami.0c23108.
66 Du F, Yener HE, Hillrichs G, Boldt R and Androsch R, *Biomacromolecules* **22**:3950–3959 (2021). https://doi.org/10.1021/acs.biomac.1c00760.
67 Du F, Rupp H, Jariyavidyanont K, Janke A, Petzold A, Binder W *et al.*, *Int J Pharm* **624**:122023 (2022). https://doi.org/10.1016/j.ijpharm.2022.122023.
68 Wong T-S, Kang SH, Tang SKY, Smythe EJ, Hatton BD, Grinthal A *et al.*, *Nature* **477**:443–447 (2011). https://doi.org/10.1038/nature10447.
69 Sprockel AJ, Khan MA, de Ruiter M, Alting MT, Macmillan KA and Haase MF, *Colloids Surf A Physicochem Eng Asp* **666**:131306 (2023). https://doi.org/10.1016/j.colsurfa.2023.131306.
70 Wang Y, Cipriani C, Hsieh C-M, Cao H, Sarmah A, Liu K-W *et al.*, *Matter* **6**:4066–4085 (2023). https://doi.org/10.1016/j.matt.2023.10.001.
71 Boskovic D and Loebbecke S, *Nanotechnol Rev* **3**:27–38 (2014). https://doi.org/10.1515/ntrev-2013-0014.

72 Thomas A, Goettmann F and Antonietti M, *Chem Mater* **20**:738–755 (2008). https://doi.org/10.1021/cm702126j.
73 Bago Rodriguez AM and Binks BP, *Curr Opin Colloid Interface Sci* **44**: 107–129 (2019). https://doi.org/10.1016/j.cocis.2019.09.006.
74 Alammar A, Kois JC, Revilla-León M and Att W, *J Prosthodont* **31**:4–12 (2022). https://doi.org/10.1111/jopr.13477.
75 Chen J, Liu X, Tian Y, Zhu W, Yan C, Shi Y *et al.*, *Adv Mater* **34**:2102877 (2022). https://doi.org/10.1002/adma.202102877.
76 Chen B, Davies R, Liu Y, Yi N, Qiang D, Zhu Y *et al.*, *Addit Manuf* **35**: 101363 (2020). https://doi.org/10.1016/j.addma.2020.101363.
77 Li X, Ouyang H, Sun S, Wang J, Fei G and Xia H, *ACS Appl Polym Mater* **5**: 2944–2955 (2023). https://doi.org/10.1021/acsapm.3c00138.
78 de Leon AC, Rodier BJ, Bajamundi C, Espera A Jr, Wei P, Kwon JG *et al.*, *ACS Appl Energy Mater* **1**:1726–1733 (2018). https://doi.org/10.1021/acsaem.8b00240.
79 Stewart KA, Lessard JJ, Cantor AJ, Rynk JF, Bailey LS and Sumerlin BS, *RSC Appl Polym* **1**:10–18 (2023). https://doi.org/10.1039/D3LP00019B.
80 Hodásová Ľ, Isarn I, Bravo F, Alemán C, Borràs N, Fargas G *et al.*, *RSC Appl Polym* **2**:284–295 (2024). https://doi.org/10.1039/D3LP00207A.
81 Smith-Jones J, Ballinger N, Sadaba N, Lopez de Pariza X, Yao Y, Craig SL *et al.*, *RSC Appl Polym* (2024). https://doi.org/10.1039/D3LP00289F.
82 Wan Z, Lee WH, Wang Y, Shegiwal A and Haddleton DM, *RSC Appl Polym* (2024). https://doi.org/10.1039/D3LP00250K.